Author Manuscript

Author Manuscript

Author Manuscript

Author Manuscript

HHS Public Access

Author manuscript

Nature. Author manuscript; available in PMC 2010 November 06.

Published in final edited form as:

Nature. 2010 May 6; 465(7294): 106–109. doi:10.1038/nature09025.

An RNA polymerase II- and AGO4-associated protein acts in RNA-directed DNA methylation

Zhihuan Gao[1,*], **Hai-Liang Liu**[1,2,*], **Lucia Daxinger**[3,*], **Olga Pontes**[4,*], **Xinjian He**[1,5], **Weiqiang Qian**[1], **Huixin Lin**[1], **Mingtang Xie**[1], **Zdravko J. Lorkovic**[6], **Shoudong Zhang**[1,5], **Daisuke Miki**[1], **Xianqiang Zhan**[1,5], **Dominique Pontier**[7], **Thierry Lagrange**[7], **Hailing Jin**[8], **Antonius J. Matzke**[3], **Marjori Matzke**[3], **Craig S. Pikaard**[9], and **Jian-Kang Zhu**[1,5]

[1]Institute for Integrative Genome Biology and Department of Botany and Plant Sciences, University of California, Riverside, CA 92521

[2]School of life science and technology, Tongji University, Shanghai 200092, China

[3]Gregor Mendel Institute of Molecular Plant Biology, Austrian Academy of Sciences, 1030 Vienna, Austria

[4]Biology Department, Washington University, Campus Box 1137, One Brookings Drive, St Louis, MO 63130

[5]Center for Plant Stress Genomics and Technology, 4700 King Abdullah University of Science and Technology, Thuwal 23955-6900, Kingdom of Saudi Arabia

[6]Max F. Perutz Laboratory, Medical University of Vienna, 1030 Vienna, Austria

[7]LGDP, CNRS/IRD/Université de Perpignan, UMR 5096, Perpignan, France

[8]Institute for Integrative Genome Biology and Department of Plant Pathology, University of California, Riverside, California 92521

[9]Department of Biology and Department of Molecular and Cellular Biochemistry, Indiana University, Bloomington, IN 47405

Abstract

DNA methylation is an important epigenetic mark in many eukaryotes1-5. In plants, 24-nt small interfering RNAs (siRNAs) bound to the effector protein, Argonaute 4 (AGO4) can direct *de novo* DNA methylation by the methyltransferase DRM22,4-6. Here we report a new regulator of RNA-directed DNA methylation (RdDM) in Arabidopsis: RDM1. Loss-of-function mutations in the *RDM1* gene impair the accumulation of 24-nt siRNAs, reduce DNA methylation, and release

Users may view, print, copy, download and text and data- mine the content in such documents, for the purposes of academic research, subject always to the full Conditions of use: http://www.nature.com/authors/editorial_policies/license.html#terms

Correspondence and requests for materials should be addressed to J.K.Z. (jian-kang.zhu@ucr.edu).
*These authors contributed equally.

'Supplementary Information accompanies the paper on www.nature.com/nature.'

Author contributions: Z.G., H.-L. L, X.H., W.Q., H.L., M.X., S.Z., D.M., and X.Z. contributed Figs 1, 2, 3b-d, supplementary figs 1-6, 9-12 and supplementary table 2. L.D, Z.J.L., A.J.M. and M.M. contributed contributed the *rdm1-4* allele (supplementary fig 5) and data on its characterization (supplementary fig 7). O.P. and C.S.P contributed fig 4, supplementary fig 8 and supplementary table 1. D.P and T.L. contributed fig 3a. J.-K.Z designed the experiments and wrote the paper together with Z.G., H.J., O.P., C.S.P. and M.M.

Author Manuscript Author Manuscript Author Manuscript Author Manuscript

transcriptional gene silencing at RdDM target loci. *RDM1* encodes a small protein that appears to bind single-stranded methyl DNA, and associates and co-localizes with RNA polymerase II, AGO4 and DRM2 in the nucleus. Our results suggest that RDM1 is a component of the RdDM effector complex and may play a role in linking siRNA production with pre-existing or *de novo* cytosine methylation. Our results also suggest that although RDM1 and Pol V may function together at some RdDM target sites in the peri-nucleolar siRNA processing center, Pol II rather than Pol V is associated with the RdDM effector complex at target sites in the nucleoplasm.

The methylation status of some loci is under dynamic control, reflecting a balance between RdDM and active demethylation mediated by the ROS1 family of DNA demethylases7-11. Loss-of-function *ros1* mutations cause DNA hypermethylation and transcriptional gene silencing (TGS) at these loci7-10. In a forward genetic screen for Arabidopsis mutations that release TGS, we recovered recessive mutations that define a new component of RdDM, RDM1 (for RNA-directed DNA Methylation 1). Silencing of the *RD29A-LUC* and *35S-NPTII* transgenes in *ros1-1*7 was suppressed or partially suppressed by the *rdm1* mutations (Figures 1A, and S1). Heavy methylation occurred at cytosines in all sequence contexts (CpG, CpNpG, and CpNpN, where N represents A, T or C) at both the endogenous and transgene *RD29A* promoters in the *ros1* mutant but methylation was reduced dramatically in the *ros1rdm1-1* plants (Figures 1B and S2). Compared to the wild-type and *ros1* plants, *ros1rdm1-1* and *rdm1-1* mutant plants had greatly diminished levels of *RD29A* promoter siRNAs (Figure 1C). The *rdm1-1* mutation abolished or substantially reduced the levels of 24-nt siRNAs from the Pol IV- and Pol V-dependent (type I) loci siRNA1003 (5S rDNA), *AtSN1*, *AtGP1*, *AtMU1* and SIMPLEHAT2, but did not affect the small RNA levels of the Pol IV-dependent but Pol V-independent (type II) loci siRNA02 and cluster 2 (Figure 2A). The *rdm1-2* mutation also dramatically reduced the level of siRNA1003 (Figure S3A). These results suggest that *RDM1* is required for 24-nt siRNAs from type I but not type II heterochromatic loci, similar to AGO4 and other components acting late in the RdDM pathway.

In wild-type and *ros1* plants, *AtSN1* elements are heavily methylated and resistant to HaeIII cleavage. The *ros1rdm1-1* and *rdm1-1* plants, like *nrpd1* plants, showed reduced methylation at *AtSN1*, such that no PCR amplification occurred following HaeIII digestion (Figure 2B). Similarly, *AtSN1* methylation was reduced in *ros1rdm1-2* compared to *ros1* and the wild type (Figure S3B). For *AtGP1*, *AtMU1*, and *AtLINE1*, wild type and *ros1* mutants showed low levels of amplification following McrBC digestion whereas *ros1rdm1-1*, *rdm1-1*, and *nrpd1* showed higher amplification (Figure 2B), indicating that methylation levels at these loci are higher in the wild type and *ros1* than in *ros1rdm1-1*, *rdm1-1*, and *nrpd1*. Southern blot analysis shows that *rdm1-1* reduces methylation at CpNpN sites of 5S rDNA (Figure 2C). At three different loci (the retrotransposon *AtSN1*, the subtelomeric repeat *MEA-ISR*, and the DNA transposon *SIMPLEHAT2*) tested by bisulfite sequencing, the *rdm1-1* mutation blocked asymmetric cytosine (CpNpN) methylation but had little or no effect on CpG methylation. The *rdm1-1* mutation also decreased CpNpG methylation at *AtSN1* and *MEA-ISR*. The effect of *rdm1-1* is similar to, or slightly stronger than, that of *ago4-1* (Figure 2D and S4A-C). Because asymmetric methylation cannot be maintained and

Author Manuscript Author Manuscript Author Manuscript Author Manuscript

thus reflects *de novo* methylation activities, these results suggest that RDM1 is critical for *de novo* DNA methylation.

Consistent with their reduced DNA methylation status, real-time RT-PCR analysis shows that *AtSN1*, *AtGP1*, *AtMU1*, and *AtLINE1* have higher expression levels in *rdm1-1* mutant than in wild-type plants (Figure 2E). RT-PCR analysis also indicated an increased expression of *AtGP1* and *AtMU1* in *ros1rdm1-2* (Figure S3C). As has been observed for *nrpd1* and other mutants in the RdDM pathway12, the *rdm1-1* mutant has a lower level of the *ROS1* transcript (Figure 2E). The Pol V-dependent transcript *AtSN1-B* is also substantially reduced in the *rdm1-1* mutant (Figure 2F).

We mapped the *rdm1-1* mutation using the loss-of-methylation phenotype at *AtSN1*, and identified a single-nucleotide-substitution mutation in At3g22680 in *rdm1-1* plants (Figures S5A and S5B). This mutation (from TAT to TAA) creates a premature stop codon, thus truncating the protein at Tyr-152 (Figure S5C). In *rdm1-2*, a 45-bp deletion in At3g22680 causes an in-frame deletion of 15 amino acid residues (Figure S5C). A T-DNA insertion mutant (FLAG_298G06) in the 5′ UTR of *RDM1*, *rdm1-3* (Figures S5B and S6A), also shows reduced DNA methylation at the *AtSN1* locus (Figure S6B). All three *rdm1* mutations cause strong reductions in the RDM1 protein level (Figures 3A and S6C). Another mutant allele, *rdm1-4*, was recovered from an independent genetic screen for mutants defective in TGS (Figure S7). The *rdm1-4* mutation also creates a premature stop codon (Figures S5B and S5C). Transformation of a 3-kb wild-type genomic fragment of At3g22680 into *ros1rdm1-1* restored silencing of the *LUC* transgene (Figure S5D) and the levels of 24-nt siRNAs and DNA methylation at the affected loci (Figures 1C, 2A-C).

The effect of the *rdm1* mutations on 24-nt siRNAs and DNA methylation is similar to that of *ago4*, suggesting that, like AGO4, RDM1 may function at a downstream step in RdDM. In the anti-Myc immunoprecipitate from Myc-AGO4 plants, we detected RDM1 protein using anti-RDM1 antibodies (Figure 3B). RDM1 was also detected in the immunoprecipitate from FLAG-DRM2 expressing plants but not from wild type plants without FLAG-DRM2 (Figure 3C). These results suggest that RDM1 associates with AGO4 and DRM2 *in vivo*. Interestingly, we found that RDM1 co-immunoprecipitates with NRPB1 of Pol II (Figure 3D), but not with NRPD1 (data not shown).

Immunostaining of RDM1 yielded fluorescence signals dispersed throughout the nucleoplasm without any preferential accumulation near the DAPI-intensive chromocenters. A prominent signal was observed at the peri-nucleolar siRNA processing center13-15 (Figure 4A). The intensity of the immunosignals was considerably weaker in the *rdm1-1* mutant (Figure 4A, bottom row), consistent with the reduced RDM1 protein level in the mutant (Figure 3A). To ascertain whether RDM1 may be co-localized with other components of the RdDM pathway, we performed double immunolocalization using the antibody specific to RDM1 in interphase nuclei from Arabidopsis transgenic lines expressing FLAG-tagged NRPD1, NRPE113 or DRM2, or Myc-tagged AGO414. Yellow signals occurring where red (NRPD1, NRPE1, AGO4 or DRM2) and green (RDM1) signals overlap reveal that RDM1 significantly overlaps with AGO4 and DRM2 in the nucleus (Figure 4B), in agreement with the co-immunoprecipitation between the proteins. The strong

Author Manuscript Author Manuscript Author Manuscript Author Manuscript

peri-nucleolar signals of NRPE1 and RDM1 also overlap, but little overlap between the two proteins is observed in the nucleoplasm. There is also negligible overlap between RDM1 and NRPD1 signals (Figure 4B). In accordance with the co-immunoprecipitation between RDM1 and NRPB1 of Pol II, we found a substantial overlap between the two proteins in the nucleoplasm (Figure 4C). Furthermore, there is also a substantial overlap between AGO4 and NRPB1 signals in the nucleoplasm (Figure 4C). We found that the AGO4 interphase pattern is altered in the *rdm1-1* mutant (Figure S8 and Table S1), suggesting that AGO4 localization is dependent on RDM1. By contrast, NRPD1 and NRPE1 maintained their typical interphase localization patterns in the *rdm1-1* mutant (Figure S8).

RDM1 appears to be highly conserved in plants, as homologous sequences are present in monocots as well as dicots (Figures S5C, S9A and S9B). This plant-specific protein has a novel fold in the protein structural space16. In the dimeric RDM1 structure (Figure S7), each monomer has a hydrophobic pocket that binds a molecule of CHAPS, a detergent used in the protein purification and crystallization16. Because CHAPS has a methyl group that appears to interact with RDM1, we tested whether RDM1 may bind to methylated DNA in electrophoretic mobility shift assays (Figure S10). Recombinant histidine-tagged RDM1 protein appeared to bind a single-stranded methyl DNA oligonucleotide containing four meCpNpN sites, but there was less binding to an unmethylated DNA oligonucleotide of the same sequence (Figures S10A-C). Mutation of RDM1 methionine-50 to alanine lessened the binding of the mutated RDM1 protein to the mCpNpN oligonucleotide (Figure S10D) and rendered RDM1 non-functional in plants (Figure S11). Chromatin immunoprecipitation results indicated that RDM1 is associated with RdDM target loci *in vivo* (Figure S12).

Our results suggest that RDM1 functions with AGO4 in the effector complex of the RdDM pathway. As the *de novo* DNA methyltransferase4, DRM2 is expected to be part of the RdDM effector complex. We observed an association and co-localization between RDM1 and DRM2, thus supporting the idea that DRM2 is indeed part of the effector complex. RDM1 appears to bind single-stranded methyl DNA. Our finding that an RdDM effector protein is capable of binding methyl DNA may help to explain how siRNA production or amplification is controlled by DNA methylation10,13,17,18. The RdDM complex may be recruited to methylated DNA through RDM1. AGO4 in the complex is known to have a slicer activity19, which presumably cuts Pol II and Pol V transcripts that are complementary to the initial trigger siRNAs. The cleaved transcript fragments could be copied by RDR2, and secondary siRNAs could then be generated by DCL3, allowing the production of more siRNAs at the methylated loci. The targeting of AGO4 to methylated DNA may also allow more efficient loading of the siRNAs generated from the methylated loci onto AGO4 to assemble into functional RdDM complexes. This suggestion is consistent with previous observations that siRNAs from already methylated DNA, but not from unmethylated DNA, can cause silencing of incoming non-methylated DNA20. As a single-stranded DNA-binding protein, RDM1 is expected to be found at sites of replication and/or transcription. The notion of RDM1 at sites of transcription is consistent with the involvement of DNA-dependent RNA polymerases Pol II, IV and V in RdDM21. Nascent transcripts generated by Pol V have been proposed to serve as scaffolds for recruiting the AGO4-containing RdDM effector complex by base-pairing with guide siRNAs22. So, it is possible that RDM1 may

Author Manuscript Author Manuscript Author Manuscript Author Manuscript

bind to single-stranded DNA at the sites of Pol V transcription. Some RdDM target sequences may be moved to the peri-nucleolar siRNA processing center where RDM1 and Pol V are co-localized (Figure 4) and may interact23. RDM1 is required for Pol V transcripts, suggesting that RDM1 may help recruit Pol V to RdDM target sites in the peri-nucleolar processing center. Importantly, RDM1 does not co-localize with Pol V in the nucleoplasm where some or the majority of RdDM target loci presumably reside. We propose that RDM1 in the nucleoplasm may bind to single-stranded DNA at the sites of Pol II transcription. This is supported by the interaction and co-localization between RDM1 and Pol II. Recently, Zheng et al21 found that Pol II plays an important role in RdDM. Our data showing AGO4 co-localization with Pol II in the nucleoplasm suggest that Pol II functions at the effector step of the RdDM pathway. By contrast, the interaction between Pol V and AGO4 appears to be restricted to the nucleolar processing center since there is a lack of co-localization between Pol V and AGO4 in the nucleoplasm13,14. The recently identified effector protein, KTF1, also co-localizes with AGO4 in the nucleoplasm24. It appears that there is a specialization of function between the scaffold transcript-producing Pol II and Pol V at different steps and/or different target loci of RdDM.

Methods summary

Mutant screening, RNA analysis, DNA methylation assays and co-immunoprecipitation experiments were carried out essentially as described in He et al11. Electrophoretic mobility shift assays were adapted from Woo et al25.

Full methods

Plant growth, mutant screening, and cloning

The wild-type plants in the C24 background carry the homozygous *RD29A-LUC* transgene26. A T-DNA mutagenized population in the *Arabidopsis thaliana ros1-1* mutant background was screened as described previously11,27. The *ros1rdm1-1* and *ros1rdm1-2* mutants were recovered from the screen. The *rdm1-1* single mutant was generated by backcrossing *ros1rdm1-1* to the wild type. The *rdm1-3* allele (FLAG_298G06) was obtained from the Arabidopsis Biological Resource Center. The *rdm1-4* allele was recovered from a different genetic screen (Figure S6). Plants were grown in a controlled room at 22°C with 16 h of light and 8 h of darkness. About 200 T_2 seedlings from each 50-line pool were screened after cold treatment (4°C, 2 days), and *RD29A-LUC* expression was analyzed as described26. A cDNA clone containing the full-length *RDM1* open reading frame was obtained from ABRC (Clone No U22863) and was cloned into Gateway vectors under the control of a dual CaMV 35S promoter for expression in transgenic plants. A 2-kb genomic fragment containing the *RDM1* promoter region was cloned into Gateway vectors pMDC164 for the promoter-GUS analysis. A 3-kb genomic fragment containing the *RDM1* open reading frame and the native promoter was amplified and cloned into vector pCAMBIA1305.1 for the complementation assay.

RNA analysis

Total RNA was extracted from Arabidopsis seedlings (14-day-old) the Trizol reagent (Sigma). A portion (30 μg) of the total RNA was loaded on a 1.0% formaldehyde gel,

Author Manuscript Author Manuscript Author Manuscript Author Manuscript

blotted to Hybond-N+ membranes. For small RNA analysis, total RNA precipitation pellets were re-suspended in 4 M LiCl; small molecular weight nucleic acids were dissolved in 4 M LiCl but high molecular weight nucleic acids remained in pellets after centrifugation. The small molecular weight nucleic acids were precipitated by an equal volume of isopropanol at -80°C overnight. About 100 μg of total nucleic acid was analyzed on a 17% polyacrylamide gel, and gels were electroblotted to Hybond N+ membranes (Amersham, Pixcataway, NJ). Membranes were cross-linked, baked for 2 hours at 80°C, and hybridized overnight at 65°C (for mRNA) or 38°C (for smRNA) with ^{32}P labeled DNA probe or oligonucleotide in PerfectHyb buffer (Sigma). Washed blots were exposed to X-ray film or a phosphorimager screen and scanned into Photoshop 7. DNA oligo probes and primers for probe amplification are listed in Supplemental Table S2.

For real-time PCR analysis, total RNA was extracted and contaminating DNA was removed with RNase-free DNase (RQ-DNase; Promega, Madison, WI). Two μg of mRNA was used for the first-strand cDNA synthesis with ThermoScript RT-PCR Systems (Invitrogen) following manufacturer's instructions. The cDNA reaction mixture was then diluted five times, and 2 μl was used as template in a 25-ml PCR reaction with iQ SYBR Green Supermix (BIO-RAD). PCR included a preincubation at 95°C for 5 min followed by 40 cycles of denaturation at 95°C for 15 s, annealing at 55°C for 30 s, and extension at 72°C for 60 s. All the reactions were carried out on the iQ5 Multicolor Real-Time PCR Detection System (BIO-RAD). The comparative threshold cycle (ct) method was used for determining relative transcript levels (Bulletin 5279, Real-Time PCR Applications Guide, BIO-RAD), using TUB8 an internal control. RT-PCR analysis of Pol V-dependent transcripts was carried out as described in reference 22. All primers used in RT-PCR and real-time PCR analysis are listed in Supplemental Table S2.

Nuclei isolation and *in vitro* transcription reactions were carried out as described28.

DNA methylation assays

Genomic DNA (500 ng) was digested with McrBC for 3 h or less. After enzyme heat inactivation at 65°C for 20 min, approximately 10% of digested DNA was used for each PCR reaction using target specific primers. PCR conditions were 2 min at 94°C followed by 35 cycles of 94°C for 30 s, 56°C for 30 s, and 72°C for 30 s. PCR products were subjected to agarose gel electrophoresis. For bisulfite sequencing, 2 μg of genomic DNA was digested with EcoRI, EcoRV, and HindIII. Digested DNA was used for bisulfite treatment using the EZ DNA methylation kit (Zymo Research, USA). Bisulfite treatment was performed in a PCR machine at 55°C for 16 h in the dark, with a jolt to 95°C for 5 min every 3 h. Bisulfite-treated DNA was purified using the EZ DNA Methylation Kit (Zymo Research, Orange, CA) following manufacturer's instructions. Purified DNA was used for amplification of endogenous and transgenic *RD29A* promoters. The PCR product was then cloned into pGEM-T easy vector (Promega). The individual clones were sequenced. Sequences of the primers are described in Supplemental Table S2.

Author Manuscript Author Manuscript Author Manuscript Author Manuscript

Electrophoretic mobility shift assay (EMSA)

The full-length *RDM1* cDNA PCR product was cloned into the pET100 vector (Invitrogen). *RDM1* mutant constructs were made using the Quickchange kit following manufacturer's instructions (Stratagene). Constructs were transformed into *E. coli* BL21(DE3) (Invitrogen) for protein expression. Recombinant proteins were purified using Ni columns (Qiagen). Methylated and unmethylated DNA oligos for the EMSA were from Integrated DNA Technologies, Inc (Caralville, IA) and were the same as used in Woo et al25. For binding assays, single-stranded or double-stranded DNA oligos (or RNA oligos) were end-labeled using T4 kinase (NEB) and radioacitive γ^{32}P ATP. Labeled DNA oligos (0.6 pmol) (or RNA oligos, or small RNAs extracted from Arabidopsis) were incubated with recombinant protein RDM1 (4 μg) in the presence or absence of cold competitors (3 pmol unless stated otherwise) in a 20 μl binding reaction. Binding reactions were carried out in 25 mM HEPES (pH 7.6), 50 mM KCl, 0.1 mM EDTA (pH 8.0), 12.5 mM $MgCl_2$, 1 mM DTT, and 5% (w/v) glycerol; 1.5 μg poly dIdC was added as a nonspecific competitor. After incubation for 45 min at room temperature, the reaction mixture was subjected to 8% PAGE with 0.5× TBE running buffer. Methylated single-stranded and double-stranded DNA oligos are listed in Supplemental Table S2.

Co-immunoprecipitation assays

Protein co-immunoprecipitation and immunoblot analysis were as described24. Anti-RDM1 antibodies were produced by injecting rabbits with purified His-tagged recombinant RDM1 protein, and were affinity-purified with RDM1 protein-conjugated resin (YenZym antibodies, South San Francisco, CA).

Immunofluorescence and microscopy

Arabidopsis leaf nuclei were extracted as described previously29 and fixed in 4% paraformaldehyde/PBS during 20 min. Prior to immunostaining, slide preparations were post-fixed in 4% paraformaldehyde/PBS and blocked with 2% BSA/PBS. Incubation with the primary antibodies was performed overnight at 4°C. The primary antibodies used to specifically detect the native proteins were as follows: rabbit anti-RDM1 (this study), chicken anti-NRPD1, chicken anti-NRPE113 and rabbit anti-AGO4 antibody, that specifically recognizes the C-terminal end of the protein. For Pol II staining, a mouse monoclonal antibody against the phosphoserine 2 version of NRPB1 (ab24758, Abcam Inc, Cambridge, MA) was used. In transgenic lines that express functional C-terminal tagged genomic versions of NRPD1, NRPE1, AGO4 or DRM2 driven by its endogenous promoter, the localization was assessed by immunolocalization of its epitope using mouse anti-Flag (Sigma) and anti-cMyc (Millipore). The detection of immunosignals was performed at 37°C for two hours using the following secondary antibodies: anti-chicken Alexa 488-conjugated (Invitrogen), anti-rabbit Alexa 488-conjugated (Invitrogen), anti-rabbit Alexa 594-conjugated (Invitrogen) and anti-mouse Alexa 488-conjugated (Invitrogen). The DNA was stained by DAPI diluted in Prolong Gold mounting media (Invitrogen).

Image stacks of nuclei were acquired with a DeltaVision restoration imaging system (Applied Precision, LLC) equipped with a CoolSnap HQ2 camera (Photometrics). The image stacks of nuclei with a Z step size of 0.20 μm were subjected to constrained iterative

Author Manuscript Author Manuscript Author Manuscript Author Manuscript

(10 iterations) deconvolution by using softWoRx software (Applied Precision). The maximum projection or the middle optical section of the deconvolved sections were merged, and processed using Adobe Photoshop 7.0 (Adobe Systems, Mountain View, CA).

Chromatin immunoprecipitation assay

Chromatin immunoprecipitation and PCR were carried out according to Gendrel et al30. Three-week-old seedlings and antibodies against recombinant RDM1 were used. PCR primers are listed in Supplemental Table S2. The anti-NRPB1 was a mouse monoclonal against the RNA polymerase II CTD repeat YSPTSPS (ab5408, Abcam Inc, Cambridge, MA).

Supplementary Material

Refer to Web version on PubMed Central for supplementary material.

Acknowledgments

This work was supported by National Institutes of Health grants (J.-K.Z.), Austrian Fonds zur Förderung der wissenschaftlichen Forschung (M.M.), National Science Foundation Career Award (H.J.), and Edward Mallinckrodt Foundation Award (O.P.). We thank Becky Stevenson for technical assistance and Tatsuo Kanno for helpful discussions.

References

1. Martienssen RA, Richards EJ. DNA methylation in eukaryotes. Curr Opin Genet Dev. 1995; 5:234–242. [PubMed: 7613094]
2. Baulcombe D. RNA silencing in plants. Nature. 2004; 431:356–363. [PubMed: 15372043]
3. Tariq M, Paszkowski J. DNA and histone methylation in plants. Trends Genet. 2004; 20:244–251. [PubMed: 15145577]
4. Chan SW, Henderson IR, Jacobsen SE. Gardening the genome: DNA methylation in Arabidopsis thaliana. Nat Rev Genet. 2005; 6:351–60. [PubMed: 15861207]
5. Matzke MA, Birchler JA. RNAi-mediated pathways in the nucleus. Nat Rev Genet. 2005; 6:24–35. [PubMed: 15630419]
6. Matzke M, Kanno T, Daxinger L, Huettel B, Matzke AJM. RNA-mediated chromatin-based silencing in plants. Curr Opin Cell Biol. 2009; 21:367–376. [PubMed: 19243928]
7. Gong Z, et al. ROS1, a repressor of transcriptional gene silencing in Arabidopsis, encodes a DNA glycosylase/lyase. Cell. 2002; 111:803–814. [PubMed: 12526807]
8. Zhu J, Kapoor A, Sridhar VV, Agius F, Zhu JK. The DNA glycosylase/lyase ROS1 functions in pruning DNA methylation patterns in Arabidopsis. Curr Biol. 2007; 17:54–59. [PubMed: 17208187]
9. Penterman J, et al. DNA demethylation in the Arabidopsis genome. Proc Natl Acad Sci USA. 2007; 104:6752–6757. [PubMed: 17409185]
10. Lister R, et al. Highly integrated single-base resolution maps of the epigenome in Arabidopsis. Cell. 2008; 133:523–536. [PubMed: 18423832]
11. He XJ, et al. NRPD4, a protein similar to the RPB4 subunit of RNA polymerase II, is a component of RNA polymerases IV and V and is required for siRNA production, RNA-directed DNA methylation, and transcriptional gene silencing. Genes Dev. 2009; 23:318–330. [PubMed: 19204117]
12. Huettel B, et al. Endogenous targets of RNA-directed DNA methylation and Pol IV in Arabidopsis. EMBO J. 2006; 25:2828–2836. [PubMed: 16724114]

Author Manuscript Author Manuscript Author Manuscript Author Manuscript

13. Pontes O, et al. The Arabidopsis chromatin-modifying nuclear siRNA pathway involves a nucleolar RNA processing center. Cell. 2006; 126:79–92. [PubMed: 16839878]
14. Li CF, et al. An ARGONAUTE4-containing nuclear processing center colocalized with Cajal bodies in Arabidopsis thaliana. Cell. 2006; 126:93–106. [PubMed: 16839879]
15. Li CF, et al. Dynamic regulation of ARGONAUTE4 within multiple nuclear bodies in Arabidopsis thaliana. PLoS Genet. 2008; 4:e27. [PubMed: 18266474]
16. Allard ST, et al. Structure at 1.6 A resolution of the protein from gene locus At3g22680 from Arabidopsis thaliana. Acta Crystallogr Sect F Struct Biol Cryst Commun. 2005; 61:647–650.
17. Slotkin RK, et al. Epigenetic reprogramming and small RNA silencing of transposable elements in pollen. Cell. 2009; 136:461–472. [PubMed: 19203581]
18. Zilberman D, et al. Role of Arabidopsis ARGONAUTE4 in RNA-directed DNA methylation triggered by inverted repeats. Curr Biol. 2004; 14:1214–1220. [PubMed: 15242620]
19. Qi Y, et al. Distinct catalytic and non-catalytic roles of ARGONAUTE4 in RNA-directed DNA methylation. Nature. 2006; 443:1008–1112. [PubMed: 16998468]
20. Chan SW, Zhang X, Bernatavichute YV, Jacobsen SE. Two-step recruitment of RNA-directed DNA methylation to tandem repeats. PLoS Biol. 2006; 4:e363. [PubMed: 17105345]
21. Zheng B, et al. Intergenic transcription by RNA Polymerase II coordinates Pol IV and Pol V in siRNA-directed transcriptional gene silencing in *Arabidopsis*. Genes Dev. 2009; 23:2850–2860. [PubMed: 19948763]
22. Wierzbicki AT, Haag JR, Pikaard CS. Noncoding transcription by RNA polymerase Pol IVb/Pol V mediates transcriptional silencing of overlapping and adjacent genes. Cell. 2008; 135:635–648. [PubMed: 19013275]
23. Law JA, Ausin I, Johnson LM, Vashisht AA, Zhu JK, Wohlschlegel JA, Jacobsen SE. Identification of a complex containing DRD1, DMS3, and RDM1, a novel protein required for Pol V-dependent transcripts. Curr Biol.
24. He XJ, et al. An effector of RNA-directed DNA methylation in *Arabidopsis* is an ARGONAUTE 4-and RNA-binding protein. Cell. 2009; 137:498–508. [PubMed: 19410546]
25. Woo HR, Pontes O, Pikaard CS, Richards EJ. VIM1, a methylcytosine-binding protein required for centromeric heterochromatinization. Genes Dev. 2007; 21:267–277. [PubMed: 17242155]
26. Ishitani M, Xiong L, Stevenson B, Zhu JK. Genetic analysis of osmotic and cold stress signal transduction in Arabidopsis: interactions and convergence of abscisic acid-dependent and abscisic acid-independent pathways. Plant Cell. 1997; 9:1935–1949. [PubMed: 9401119]
27. Kapoor A, et al. Loss-of-function mutations in a conserved replication protein suppress transcriptional gene silencing in a DNA methylation-independent manner in Arabidopsis. Curr Biol. 2005; 579:5889–5898.
28. Dorweiler JE, et al. Mediator of paramutation1 is required for establishment and maintenance of paramutation at multiple maize loci. Plant Cell. 2000; 12:2101–2118. [PubMed: 11090212]
29. Jasencakova Z, Meister A, Walter J, Turner BM, Schubert I. Histone H4 acetylation of euchromatin and heterochromatin is cell cycle dependent and correlated with replication rather than with transcription. Plant Cell. 2000; 12:2087–2100. [PubMed: 11090211]
30. Gendrel AV, Lippman Z, Yordan C, Colot V, Martienssen RA. Dependence of heterochromatic histone H3 methylation patterns on the Arabidopsis gene DDM1. Science. 2002; 297:1871–1873. [PubMed: 12077425]
31. Kanno T, et al. A structural-maintenance-of-chromosomes hinge domain-containing protein is required for RNA-directed DNA methylation. Nat Genet. 2008; 40:670–675. [PubMed: 18425128]
32. Daxinger L, et al. A stepwise pathway for biogenesis of 24-nt secondary siRNAs and spreading of DNA methylation. EMBO J. 2009; 28:48–57. [PubMed: 19078964]

Author Manuscript Author Manuscript Author Manuscript Author Manuscript

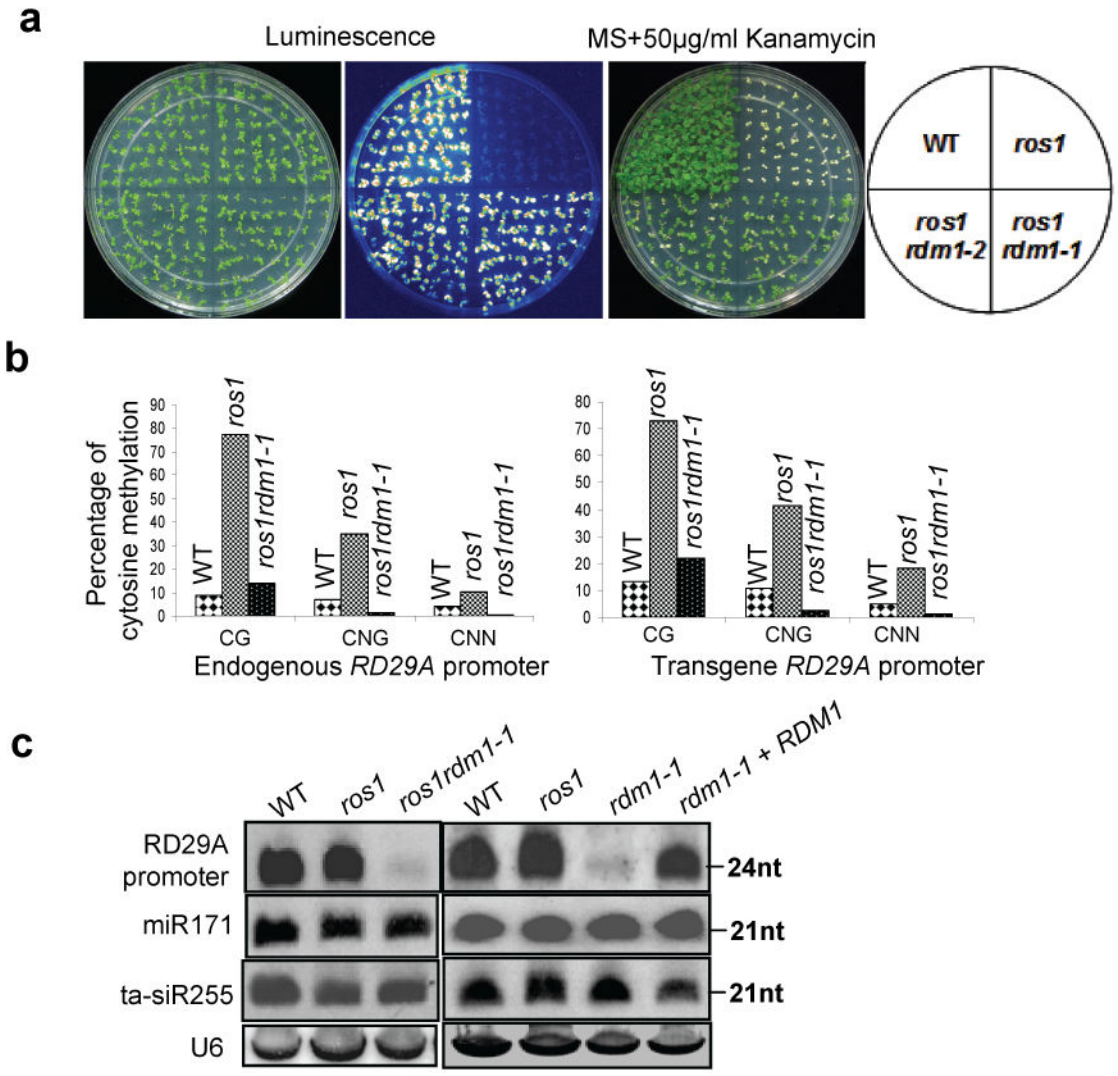

Figure 1. Effects of *rdm1* on *RD29A-LUC* and *35S-NPTII* silencing, DNA methylation and small RNAs

a, Effects of *rdm1* on *RD29A-LUC* and *35S-NPTII* silencing as indicated by luciferase activity and kanamycin resistance of the *ros1rdm1* mutants. Wild type (WT), *ros1*, *ros1rdm1-1* and *ros1rdm1-2* were grown for 10 days and imaged after cold treatment (48 h, 4°C). For kanamycin resistance test, the seeds were planted on MS medium supplemented with kanamycin (50 mg/l). Seedlings were photographed after 2 weeks. **b**, Methylation status of the endogenous and transgene *RD29A* promoter as determined by bisulfite sequencing. c, Detection of small RNAs in WT, *ros1*, *rdm1-1* single mutant, *ros1rdm1-1* double mutant, and a *rdm1-1* complementation line (*rdm1+RDM1*; T3 generation).

Author Manuscript Author Manuscript Author Manuscript Author Manuscript

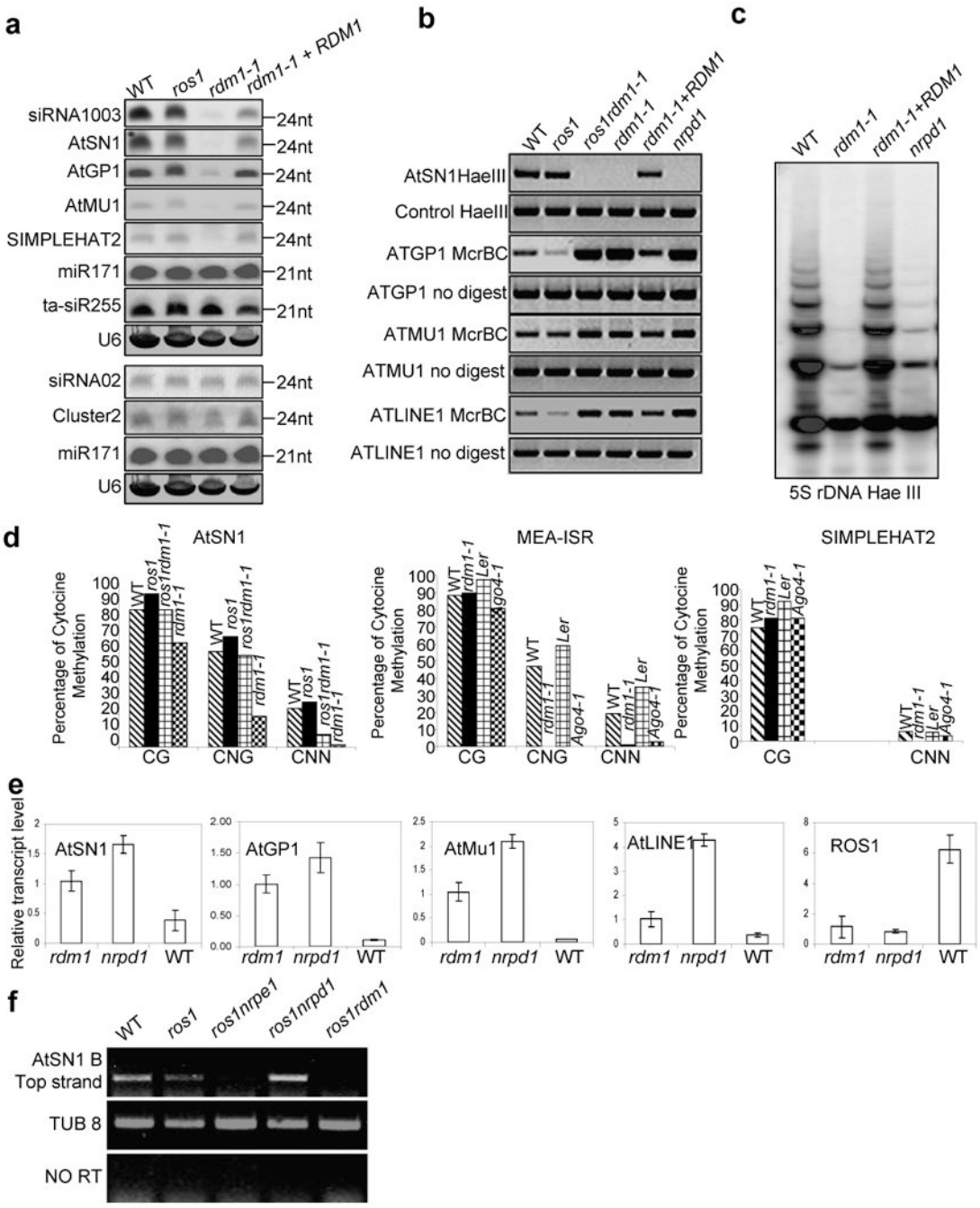

Figure 2. Effects of *rdm1-1* on siRNA and transcript levels and DNA methylation at endogenous RdDM target loci

a, Detection of various small RNAs. U6 snRNA was used as loading control. The positions of size markers are indicated (24 nt or 21 nt). **b**, DNA methylation status as determined by PCR-based assays. The At2g19920 gene, which lacks HaeIII sites, served as a PCR control for *AtSN1*. The same amounts of undigested DNA from different samples were used as controls for *AtGP1*, *AtMu1*, and *AtLINE1*. PCR cycles were 35 and 30, respectively, for McrBC digested and undigested samples. **c**, Southern blot analysis of the methylation status

Author Manuscript Author Manuscript Author Manuscript Author Manuscript

of 5S rDNA repeats using genomic DNA digested with the methylation-sensitive enzyme HaeIII. **d**, Methylation status of *AtSN1*, *MEA-ISR*, and *SIMPLEHAT2* as determined by bisulfite sequencing. **e**, Determination of transcript levels by real-time RT-PCR. The transcript levels were normalized using *TUB8* as an internal standard. Error bars represent S.D. (n=3). **f**, RT-PCR analysis of a Pol V-dependent transcript from *AtSN1*. *TUB8* was amplified as an internal control. PCR reactions without reverse transcription (NO RT) were carried out as controls to rule out DNA contamination.

Author Manuscript Author Manuscript Author Manuscript Author Manuscript

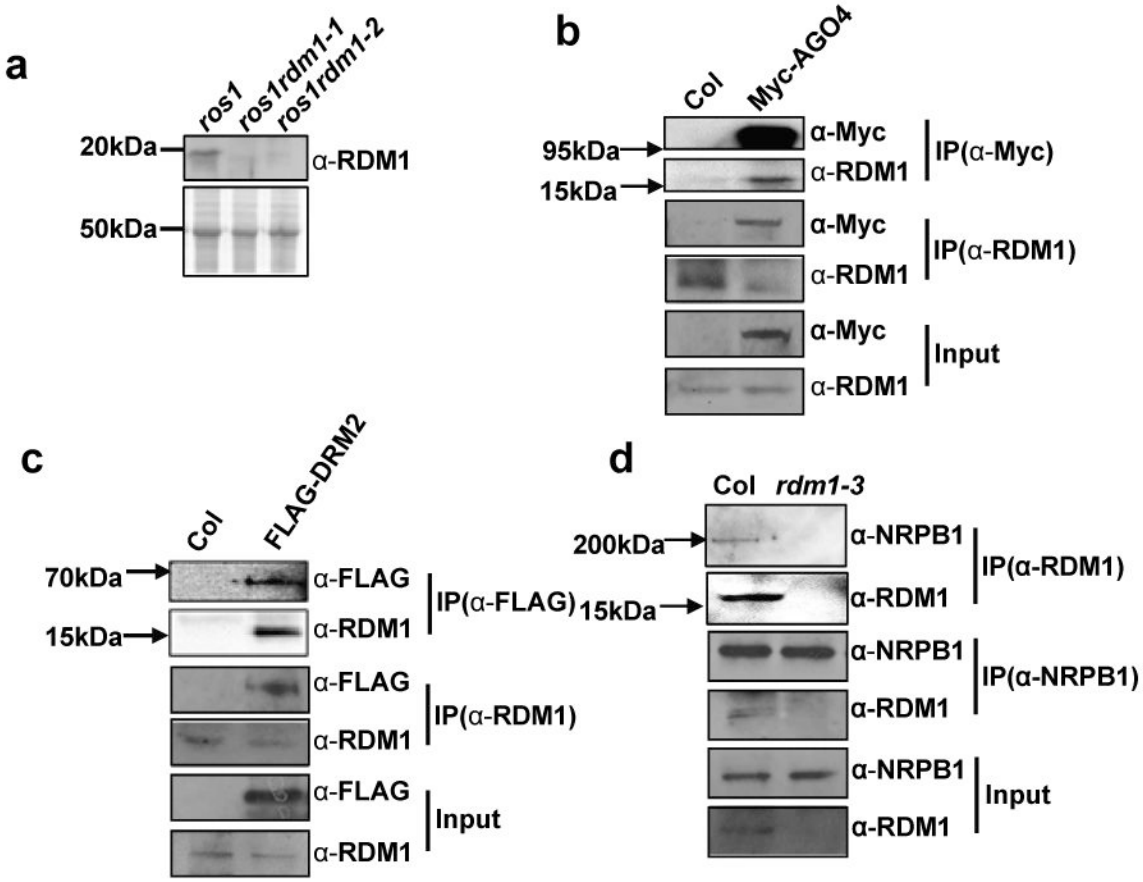

Figure 3. Immunoblot analysis of RDM1 and its interaction with AGO4, DRM2 and NRPB1

a, Western blot analysis of RDM1 protein levels. Coomassie-stained gel (lower panel) is shown as control for loading. **b**, Co-immunoprecipitation between Myc-AGO4 and RDM1. **c**, Co-immunoprecipitation between FLAG-DRM2 and RDM1. **d**, Co-immunoprecipitation between NRPB1 and RDM1.

Author Manuscript Author Manuscript Author Manuscript Author Manuscript

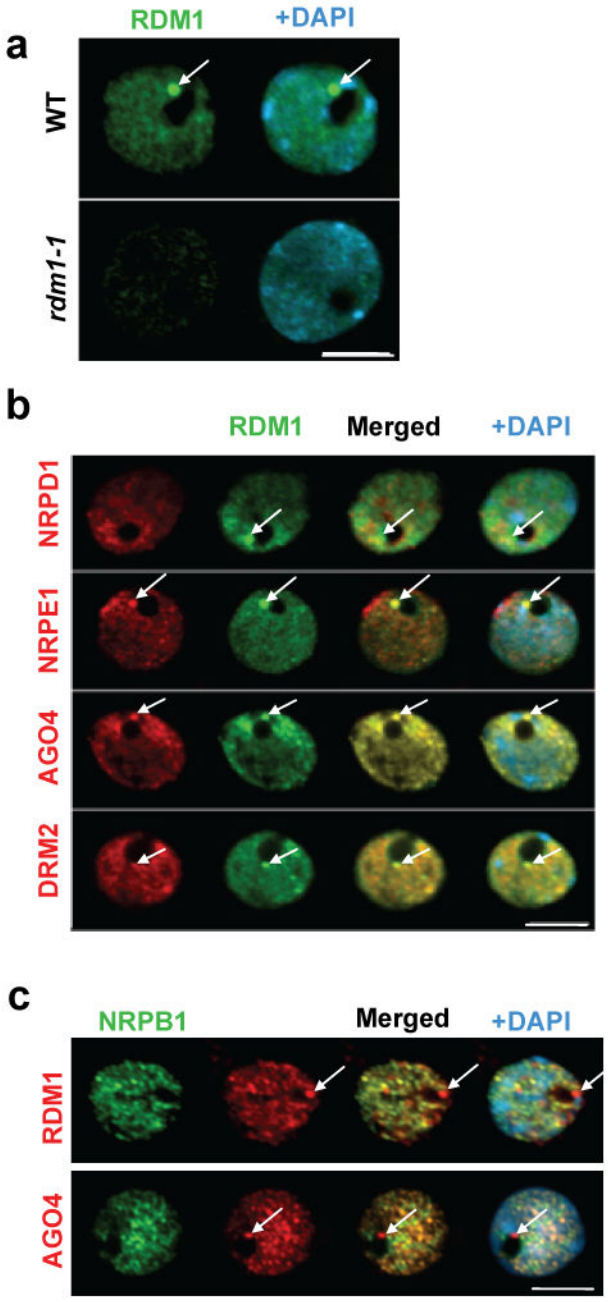

Figure 4. Sub-nuclear localization of RDM1 and its co-localization with other components of the RdDM pathway

a, The nuclear distribution of RDM1 was analyzed by immunostaining using anti-RDM1 (green). **b**, Dual immunolocalization using anti-RDM1 (green) in transgenic lines expressing recombinant full-length epitope tagged FLAG-NRPD1, Myc-AGO4, FLAG-NRPE1 and FLAG-DRM2 (red). **c**, Dual immunolocalization using anti-NRPB1 and anti-RDM1 or anti-AGO4. In all panels the DNA was stained with DAPI (blue) and the size bars correspond to 5 μm. Arrows point to the peri-nucleolar dot (siRNA processing center).